Fall 2009

The role of ozone forcing on climate models

Sium Tesfai Gebremariam

THE ROLE OF OZONE FORCING ON CLIMATE MODELS

A Thesis

Presented to

The Faculty of the Department of Meteorology

San José State University

In Partial Fulfillment

of the Requirements for the Degree

Master of Science

by

Sium Tesfai Gebremariam

December 2009

SAN JOSE STATÉ UNIVERSITY

The Undersigned Thesis Committee Approves the Thesis Titled

THE ROLE OF OZONE FORCING ON CLIMATE MODELS

by

Sium Tesfai Gebremariam

APPROVED FOR THE DEPARTMENT OF METEOROLOGY

Dr. Eugene C. Cordero	Department of Meteorology	Date
Dr. John Abatzoglou	Department of Meteorology	Date
Dr. Steven A. Mauget	USDA/ Agricultural Research Service, Plant Stress and Water Conservation Laboratory	Date

APPROVED FOR THE UNIVERSITY

Associate Dean	Office of Graduate Studies and Research	Date

ABSTRACT

THE ROLE OF OZONE FORCING ON CLIMATE MODELS

by Sium Tesfai Gebremariam

Thirteen coupled Atmospheric Oceanic Global Circulation Models (AOGCMs) and seven Chemistry Climate Models (CCMs) are compared to radiosonde and satellite observations to assess model performance and to study the connection between ozone forcing and model temperature trends during the last two decades. Overall, CCMs and AOGCMs that include time-varying ozone forcing agree reasonably well with observations in the lower stratosphere for both annual and seasonal averages, but models without time-varying ozone forcing (fixed) are statistically different from observations between ~ 150 hPa and 10 hPa. Both CCMs and those AOGCMs with time-varying ozone forcing capture the seasonality of the observed southern hemisphere extratropical lower stratospheric temperature trends. In the tropical lower stratosphere, only a few models show seasonal temperature trend variations that resemble the observations. In the middle troposphere (500 hPa), significant differences between models and observations were found, both in the tropics (during DJF and JJA) and in the southern hemisphere extratropics (during MAM and JJA). These differences are difficult to reconcile, although our analyses indicate that the inclusion of stratospheric ozone forcing may affect trends from the stratosphere down into the troposphere.

ACKNOWLEDGEMENTS

I would like to offer my sincerest gratitude to my advisor, Dr. Eugene Cordero, for his guidance and support that helped me to complete my studies. I am also grateful to him for giving me the opportunity to work with him and broaden my scientific horizon. Discussing and working with him was a productive and extraordinary experience for me.

I sincerely thank members of my thesis committee, Dr. John Abatzoglou and Dr. Steven A. Mauget. Their critical comments helped to improve my thesis. I also would like to thank all the faculty members of the department for providing me with an excellent meteorology background.

Many thanks go to my wife Sabine Niklas for her encouragement, understanding and patience while I completed my degree abroad. I dedicate my thesis to her and our children Helen and David.

Finally, I would like to particularly extend my thanks to Clare Cordero for editing my thesis, Bereket Lebassi for providing me with constant encouragement and personal support in numerous ways, and Shoukri Kasakseh for being a true friend. In addition, I am grateful for the support and friendship I received from my fellow students.

This research was supported by NSF's Faculty Early Career Development program, Grant ATM-00449996 and NASA's Living with a star, Targeted Research and Technology Program, Grant LWS04-0025-010.

TABLE OF CONTENTS

LIST OF TABLES

LIST OF FIGURES

1. Introduction

Stratospheric climate is influenced by coupled changes in atmospheric dynamics, chemical composition, and radiative processes. Chemical reactions affect atmospheric dynamics through radiative heating while the dynamics affect chemical reactions through transport processes (Eyring et al. 2006). Numerical model results show that stratospheric dynamics are sensitive to changes in greenhouse gases (GHGs), the solar cycle, perturbations due to volcanic aerosols and ozone depletion (e.g., Butchart and Scaife 2001; Butchart et al. 2006). For example, Li et al. (2008) using a coupled chemistry climate model found an increase of upward mass flux in the lower stratosphere was due largely to ozone depletion (approximately 60% increase) while the rest was due to increases in GHGs, the solar cycle and volcanic aerosols during the 20^{th} century. An increase in upward mass flux influences the net mass exchange between the troposphere and stratosphere which in turn affect the large scale stratospheric circulation. Thus, understanding how these interactions are changing is important for quantifying long-term changes in stratospheric and tropospheric climate (IPCC 2007; WMO 2007).

Over the last two decades, modeling and observational studies have worked to identify how declines in stratospheric ozone and increases in GHGs affect stratospheric temperature. Ramaswamy and Schwarzkopf (2002) found that most of the annual mean stratospheric cooling during 1979-2000 was due to the combined effects of stratospheric ozone depletion and increases in GHGs. Randel and Wu's (1999) observational analysis found lower stratospheric cooling associated with ozone depletion in both the Arctic and

the Antarctic, with the larger decreases occurring in Antarctica during late winter and early spring.

Recent studies have also identified an apparent link between changes in the stratosphere and changes in the troposphere. The observational analysis of Thompson and Solomon (2002) and the modeling work of Gillett and Thompson (2003) both suggest that stratospheric ozone changes are connected with the surface temperature trends over Antarctica. In particular, cooling over most of the Antarctic continent and warming over the Antarctic Peninsula are associated with an acceleration of westerly winds in the troposphere (due to the enhanced meridional temperature gradient between polar regions and midlatitudes). Studies have also suggested that observed increases in the southern annual mode (SAM) index are linked to changes in GHGs and ozone depletion (e.g., Fyfe et al. 1999; Kushner et al. 2001; Gillett and Thompson 2003; Marshall 2003), as well as cooling of interior Antarctica and warming in Antarctic Peninsula. However, recent evidence by Steig et al. (2009) show an overall warming of Antarctica continent with significant warming in the western part of Antarctica ($> 0.1^0$C decade^{-1} over the past 50 years) and cooling in the eastern Antarctica due to the regional atmospheric circulation changes and its associated change in sea surface temperature and sea ice. Furthermore, both observational and modeling studies showed a decrease in stratospheric geopotential heights, which extend down to the surface over Antarctica (Thompson and Solomon 2002; Gillett and Thompson 2003). Most recently, Karpechko et al. (2008) found that only those coupled Atmospheric Oceanic General Circulation Models (AOGCMs) that include ozone forcing and a high vertical resolution in the lower

stratosphere accurately simulated the observed decreases in the geopotential height and temperature trends throughout the Antarctic troposphere. These results indicate that stratospheric ozone depletion may have an impact on the tropospheric climate although the mechanisms explaining these interactions remains unclear (Thompson et al. 2006; Nathan and Cordero 2007; WMO 2007).

a. Model intercomparison studies

Various studies of the stratosphere and its role on climate have focused on assessing model performance and the intercomparison of models (e.g., Pawson et al. 2000; Austin et al. 2003; Cordero and Forster 2006; Eyring et al. 2006 and references therein). Shine et al. (2003) conducted a multi-model CCM comparison focusing mainly on the global and annual-mean lower stratospheric temperature trends over the last two decades (1980-2000). Although their results generally showed good agreement between models and observations, in the northern hemisphere midlatitudes at 50 hPa, the models underestimated the cooling compared to observations. The study also noted that the differences between models and observations at 50 hPa would be reduced if the effect of water vapor changes were accounted for.

Likewise, Cordero and Forster (2006) performed a model intercomparison using observational datasets from satellite, radiosonde and AOGCM models that contributed to the 2007 Intergovernmental Panel on Climate Change Fourth Assessment Report (IPCC AR4). Their analysis found significant differences between models and observed temperature trends in the upper tropical troposphere over the last three decades. These

differences were found to be larger in models that did not include 20th century ozone depletion.

Following Cordero and Forster (2006), both coupled AOGCMs and CCMs are compared to radiosonde and satellite observations to assess model performance and to study the connection between ozone forcing and model temperature variability and trends. Different from the above model assessments, both AOGCMs and CCMs are compared to examine whether there is a systematic difference between these groups of models and to investigate the role of interactive chemistry on temperature trends. To accomplish this, annual and seasonal temperature trends in the stratosphere and troposphere are compared to updated radiosonde and satellite observations. Understanding how ozone changes affect temperature trends in the lower stratosphere and upper troposphere may be important to help resolve differences between models and observations in the tropical upper troposphere (Cordero and Forster 2006; Lanzante and Free 2008).

In Section 2, a brief description of the observational and model temperature datasets is given, along with the various methods of analysis. The results are given in Section 3, where a detailed comparison between models and observations is given. The comparisons between models and both radiosonde and satellite observations are done for different regions, seasons and vertical levels. A discussion and summary are provided in Section 4.

2. Data and methodology

a. Radiosonde observations

Monthly averaged radiosonde temperatures obtained from the Radiosonde Atmospheric Temperature Products for Assessing Climate (RATPAC) are available since 1958. These datasets are developed from 87 stations that are somewhat uniformly distributed around the global, although fewer measurements exist in the southern hemisphere and tropics.

The datasets originally contained inhomogeneities due to variations in measurement conditions (e.g., change in instrument, time of observation). Over the last few decades, efforts were made to reduce the inhomogeneities of these data, including the temporal homogenization of the RATPAC datasets from 1958-1997 performed by Lanzante et al. (2003a; 2003b) and are often referred to as LKS adjusted datasets. Using the adjusted LKS data extending over the period of 1958-1995 from 85 out of 87 stations, RATPAC datasets have been expanded and updated on a monthly basis using the first difference method and they cover monthly mean temperature data extending from the surface through 30 hPa pressure levels. The RATPAC data at 10 and 20 hPa pressure levels are often excluded due to the scarcity of the temperature datasets at these two levels (Peterson et al. 1998; Free et al. 2005).

Several studies have analyzed the RATPAC datasets (Parker et al. 1997; Angell 2000; Gaffen et al. 2000) and compared this climatology with other observational datasets such as from satellites (Christy et al. 2000; Hurrell et al. 2000; Lanzante et al. 2003b) and NCEP and ERA40 reanalysis data (Santer et al. 2003a; Santer et al. 2003b).

Randel and Wu (2006) compared the adjusted LKS radiosonde data with Microwave Sounding Unit (MSU) satellite data and found significant differences in the tropical lower stratosphere. These differences were attributed to instrument changes in various tropical radiosondes and it was suggested that these be removed from the climatology. Thus a new RATPAC climatology (hereafter referred to as RATPAC47) shown in Fig. 1 was developed using only 47 stations that agreed with the satellite observations since 1979 (Randel et al. 2009). Thus, in this paper we utilize the RATPAC47 dataset for the temperature trend analysis.

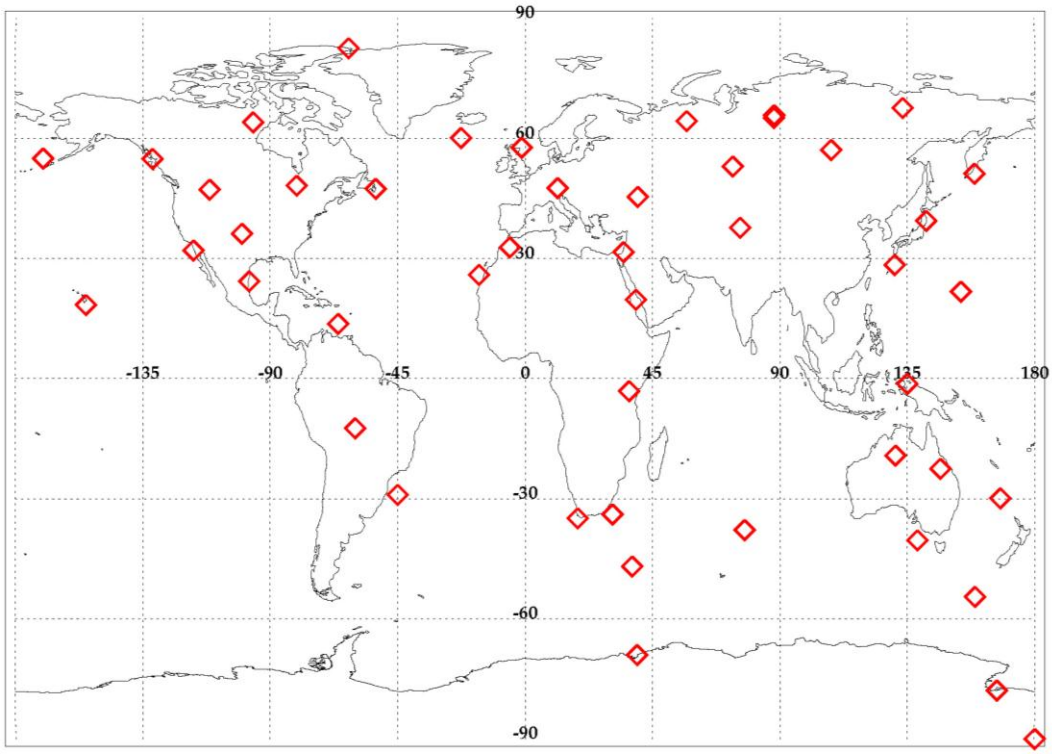

Fig. 1. Location of the 47 radiosonde stations (red diamond symbols).

b. Satellite observations

The MSU temperature data obtained from the NOAA polar-orbiting satellites are available since 1979 and measure temperatures in atmospheric layers in the lower and middle troposphere and the lower stratosphere. Although both observational datasets (radiosonde and satellite) are global in their coverage, the satellite data has much better horizontal coverage. The satellite temperature data used in this study are MSU channel 2 (lower and middle troposphere, surface to ~ 18 km), and MSU channel 4 (lower stratosphere, ~13-22 km), obtained from the Remote Sensing System (Christy et al. 2000; Mears et al. 2003).

c. AOGCMs and CCMs datasets

The output from 23 AOGCMs simulations of the 20th century requested by the 2007 IPCC AR4 have been completed and archived at the Program for Climate Model Diagnosis and Intercomparison. Likewise, model simulations from 13 CCMs for the 20th and 21st century have been archived at the British Atmospheric Data Centre for use in the 2006 WMO Ozone Assessment (Eyring et al. 2006; Meehl et al. 2007). Although different numbers of model runs were performed by changing the initial conditions only, Run 1 AOGCMs simulations and Reference simulations 1 (REF1) from CCMs simulations (Eyring et al. 2005) were used.

From the AOGCMs that participated in the IPCC AR4, 18 models contributed A2 emission scenario runs that extend into the 21st century, although we restricted our analysis to the 13 models that included realistic stratospheric simulations. In order to

extend the length of the comparison between AOGCMs, CCMs, and observations, the AOGCMs A2 scenario has been combined with the 20th century simulations. This allows trend analysis between 1980 and 2004. Likewise, 5 out of 13 REF1 CCMs used in this study have simulations between 1980 and 2004, and we also included the WACCM and GEOSCCM simulations from 1980 to 2003. Five of the CCMs (E39C, UMETRAC, UMSLIMCAT, MAECHAM4CHEM and LMDZrepro) have simulations between 1980 and 1999 (Eyring et al. 2006) and are not included. In addition, the ULAQ model was not included due to the poor model representation of the upper tropospheric dynamics (Butchart et al. 2009). Therefore, the main constraint on the number of models used in this study (7 CCMs and 13 AOGCMs) was the availability of temperature datasets during the last two decades.

The main focus of this paper is to analyze the monthly and zonally-averaged mean temperature data from the AOGCMs, and CCMs and compare them with observations. The comparison of trends is conducted from the surface to 10 hPa since this is the range of output requested by the IPCC. Moreover, significant differences between these groups of models exist. While both types of models contain an atmospheric general circulation model, the CCMs also contain interactive chemistry built in to incorporate various existing atmospheric chemical reactions that interact self consistently with the radiation and dynamics. However, the CCMs do not contain an ocean model and instead use time-varying prescribed sea surface temperature from observations [e.g., HadISST1 (Rayner et al. 2003)] and calculate the ozone fields within the model. The AOGCMs contain interacting atmospheric ocean models, but require

existing chemical fields such as either fixed or time-varying ozone forcing to be prescribed (Eyring et al. 2006; WMO 2007). In addition, each individual model may differ not only in its inclusion of forcing (Cordero and Forster 2006) but also in relation to other factors (e.g., vertical and horizontal resolution). About half of the AOGCMs have model levels that extend above 10 hPa, while most (12/13) of the CCMs extend above 10 hPa. The vertical and horizontal resolution of CCMs along with the forcing employed in the models are described (together with references) by Eyring et al. (2006) while similar descriptions for AOGCMs domain resolution and forcing can be found in Meehl et al. (2007) and references therein.

d. Model analysis

The above-mentioned models and observations datasets are used to perform temperature trend analysis and comparison for different seasons and different regions. The names, abbreviations and latitude ranges of each of the four regions are: Global (GL) 90^{o}S-90^{o}N, tropics (TR) 30^{o}S-30^{o} N, southern hemisphere extratropics (SHextra) 30^{o}S-90^{o}S, and northern hemisphere extratropics (NHextra) 30^{o}N-90^{o}N. This analysis is performed both for the annual and seasonal trends, where the seasonal temperature trends are computed by averaging 3 months (i.e., for December through February (DJF), March through May (MAM), June through August (JJA), and September through November (SON).

Temperature trends are computed for each model and observation for the period 1980-2004. Trend values are calculated throughout the paper from a linear least square

analysis with trend uncertainties computed using the standard error, where autocorrelation is employed to account for non randomness of temperature data (Santer et al. 1999; Wigely et al. 2006). In addition, the AOGCMs are separated depending on their inclusion of stratospheric ozone trends, where models that include a time-varying ozone forcing are referred to as AOGCMs-O_3 (8/13), the models with a fixed ozone forcing are referred to as AOGCMs-NO_3 (5/13) and CCMs (7) models (see Table 1). After separating and categorizing the models based on the inclusion of ozone forcing, temperature trends are computed for the grouped and averaged models. Finally, the standard deviation from the averaged models is evaluated to examine the model-to-model variability from the surface to 10 hPa.

To investigate how well each individual and the average models simulate the observed temperature trends, they are compared to the observations to determine if the model simulated trend and the observed trend are statistically similar. This is done by computing the difference of the model with the observed time series and evaluating the trend of that difference (Wigely et al. 2006). If the trend in the difference is statistically different from zero, then there is a statistical difference (at the 95% confidence level) between the model and the observations.

Table 1. Models categorized based on their inclusion of ozone forcing. "Yes" means time-varying ozone forcing are prescribed in the models, and "NO" means fixed (without time-varying) ozone forcing are prescribed in the models. CCMs evaluate ozone forcing within the models and are denoted by "Calculated".

Models	Ozone Forcing	Country of origin	Group of models
CCSM3	Yes	Canada	AOGCMs-O_3
CSIRO-MK3.0	Yes	Australia	
ECHAM5-MPI-OM	Yes	Germany	
GFDL-CM2.0	Yes	USA	
GFDL-CM2.1	Yes	USA	
GISS-ER	Yes	USA	
PCM	Yes	USA	
UKMO-HADCM3	Yes	UK	
CGCM3.1-T47	NO	Canada	AOGCMs-NO_3
CNRM-CM3	NO	France	
BCCR-BCM2.0	NO	Norway	
INM-CM3.0	NO	Russia	
IPSL-CM4	NO	France	
AMTRAC	Calculated	USA	CCMs
CCSRNIES	Calculated	Japan	
CMAM	Calculated	Canada	
GEOSCCM	Calculated	USA	
MRI	Calculated	Japan	
SOCOL	Calculated	Switzerland	
WACCM	Calculated	USA	

The simulated annual and seasonal temperature trends are also compared with the MSU satellite data both in the middle troposphere (TMT) and the lower stratosphere (TLS). Since the satellite measures layered atmospheric temperatures derived from measurement of the absorption of microwave oxygen molecule, weighting functions for the MSU2 and MSU4 satellite datasets (see Table 2) are applied both to the models (i.e., AOGCMs-O_3, AOGCMs-NO_3 and CCMs) and to the radiosonde observations to produce satellite analogous time series for the TMT and TLS. Models and radiosonde latitude ranges are slightly modified to match the satellite latitude ranges, where they are defined

as global (GL) 82.5°S-82.5°N, tropics (TR) 20°S-20° N, southern hemisphere extratropics (SHextra) 20°S-82.5°S, and northern hemisphere extratropics (NHextra) 20°N-82.5°N. In addition, time series differences between models and satellite observations are also produced to examine if there is a statistically significant difference between models, radiosonde and satellite observations.

Table 2. Weighting functions for the MSU2 and MSU4 satellite datasets over land as applied to the models and RATPAC47 datasets.

	Models		RATPAC	
Pressure (hPa)	TMT	TLS	TMT	TLS
1000	0.11	0.00	0.12	0.00
925	0.04	0.00	0.00	0.00
850	0.07	0.00	0.09	0.00
700	0.10	0.00	0.15	0.00
600	0.10	0.00	0.00	0.00
500	0.12	0.00	0.17	0.00
400	0.13	0.00	0.13	0.00
300	0.09	0.00	0.09	0.00
250	0.06	0.00	0.06	0.00
200	0.06	0.03	0.06	0.03
150	0.05	0.12	0.05	0.12
100	0.04	0.23	0.04	0.23
70	0.02	0.23	0.02	0.23
50	0.01	0.19	0.01	0.19
30	0.01	0.11	0.01	0.19
20	0.00	0.05	0.00	0.00
10	0.00	0.03	0.00	0.00
Sum	1.00	1.00	1.00	1.00

3. Results

This section compares how well the models simulate the observed annual mean temperature trends computed between 1980 and 2004 for four latitude ranges (global, tropics, northern hemisphere extratropics and southern hemisphere extratropics) between the surface and 10 hPa. First individual model temperature trends are compared with the observed radiosonde trends, then the model-to-model variability as a function of pressure in the above mentioned four regions are analyzed.

a. Radiosonde observations

The observed annual mean vertical temperature trends plotted in Fig. 2 show warming in the troposphere and cooling in the stratosphere, similar to previous studies (e.g., Santer et al. 2005; Cordero and Forster 2006; Eyring et al. 2006). In the middle stratosphere (between 50 hPa and 10 hPa), observations show the largest annual mean cooling trends in the tropics compared to other regions.

Figure 2 also illustrates how in the observations, the annual mean SHextra temperature trends have cooled more than the NHextra, especially between 200 hPa and 50 hPa. Another difference between the NHextra and SHextra is the temperature trend variation with height in the stratosphere (Fig. 2c and Fig. 2d). While observations show cooling trend between 100 hPa and 30 hPa in both hemisphere extratropics, in the NHextra the cooling trend increases with height whereas in the SHextra the cooling trend is nearly constant between 70 hPa and 30 hPa. For example, the cooling trend in the

NHextra and SHextra changed from 70 hPa to 50 hPa by 0.2 K decade^{-1} and 0.05 K decade^{-1}, respectively.

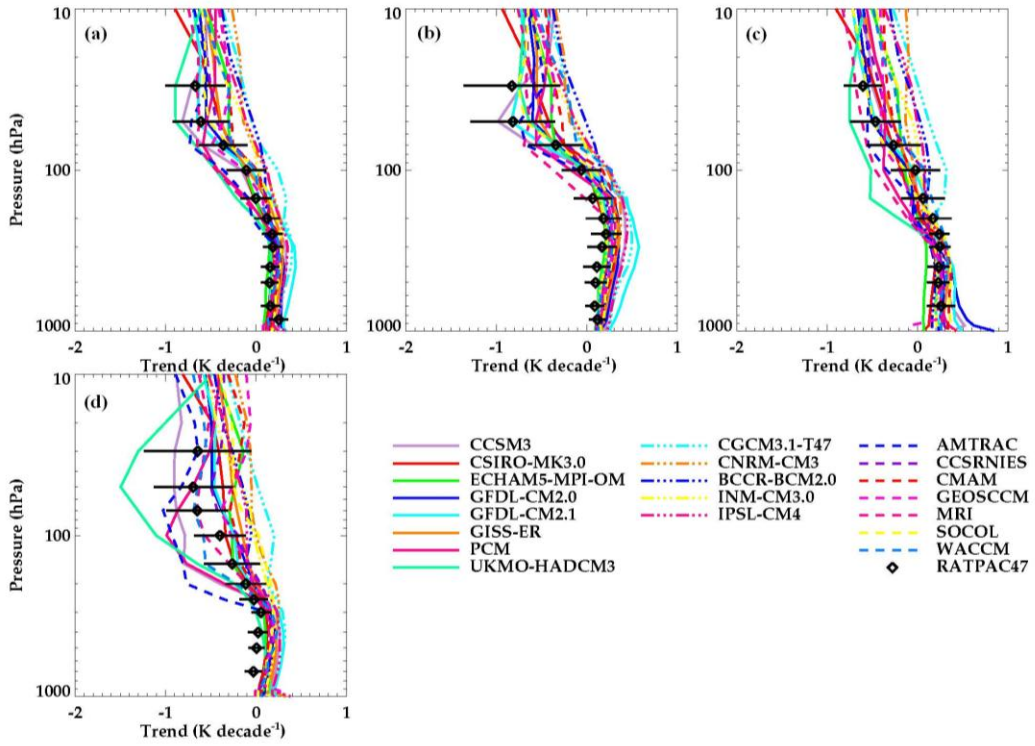

Fig. 2. Annual mean temperature trends from 1980-2004 for (a) global, (b) tropics, (c) NHextra, and (d) SHextra. Each climate model (AOGCMs and CCMs) is represented by colored lines, with AOGCM-O_3 models shown by the colored solid lines, the AOGCM-NO_3, and the CCMs by the colored dashed lines and dotted-dashed lines, respectively. The RATPAC47 observations are represented by black diamond symbols and the two-sigma uncertainties are indicated by a black horizontal line.

The larger ozone loss in the SHextra compared to the NHextra is likely the explanation for the hemispheric difference in the vertical structure of the temperature trends. In the troposphere, observations show larger tropospheric warming trends (between 0.2 K decade^{-1} and 0.3 K decade^{-1}) in the NHextra, compared to other regions, while in the SHextra, observations show negligible trends between surface and 300 hPa.

An explanation for the weak trends in the SHextra may be related to the sparse radiosonde sampling in the southern hemisphere (Lanzante and Free 2008), although this is not clear.

Further information about the observed trends can be found by examining the 2-sigma (95 %) confidence interval in the observations. The trend confidence interval is about twice as large in the stratosphere compared to the troposphere. For example, the global annual mean trend confidence interval at 50 hPa is 0.31 K decade^{-1} whereas at 500 hPa and 850 hPa, they are about 0.11 K decade^{-1}. The largest confidence interval is observed in both the tropics and SHextra at 70 hPa, 50 hPa and 30 hPa pressure levels. The observational confidence interval is also larger in the SHextra, compared to the NHextra in the upper troposphere and lower stratosphere (between 200 hPa and 30 hPa). For example, the confidence interval at 50 hPa in the SHextra (0.44) is about 35 % larger than the NHextra (0.28). This larger confidence interval in the stratosphere indicates that the stratosphere is subject to larger variability than the troposphere due to volcanic aerosols and solar activity.

b. Model simulations

Models and radiosonde observations (Fig. 2) generally show similar vertical temperature trend profiles, although there are significant differences. For example, models show different shape of tropospheric warming and stratospheric cooling in the global mean, tropics, NHextra and SHextra. In the stratosphere, the AOGCMs-NO_3 generally underestimate the observed stratospheric cooling (due to the absence of the

change in the ozone forcings in these models) while both AOGCMs-O_3 and CCMs appear to show reasonable cooling trends with some exceptions. A few AOGCMs-O_3 (PCM and UKMO-HADCM3) and CCMs (AMTRAC and MRI) appear to overestimate the global annual mean cooling trends at the pressure levels between ~150 hPa and 70 hPa. This is likely due to over prescribed or calculated ozone loss in the stratosphere although we do not have information about the AOGCMs ozone fields. However, as noted by Eyring et al. (2007), AMTRAC and MRI CCMs over predict ozone losses due to enhanced inorganic chlorine and this partially explains the larger cooling trends in the stratosphere.

Both the GFDL-CM2.0 and GFDL-CM2.1 models show an overestimation of the tropospheric warming between 850 hPa and 300 hPa, and up to 150 hPa in the case of the tropics (Fig. 2a, b and d). These results are similar to the findings of Lanzante and Free (2008) who compared a subset of AOGCMs with radiosonde observations over both the radiosonde era (1960-1999) and the satellite era (1979-1999). Moreover, the GFDL-CM2.0 model shows the largest warming trends at the surface in the NHextra (Fig. 2c) and the ECHAM5-MPI-OM model shows almost constant warming (though not statistically significant) trends from the surface to ~ 250 hPa. The shortcomings of the two versions of GFDL-CM models have been related to the larger ENSO amplitudes (Lanzante and Free 2008).

Another way of characterizing model variability is to study the model-to-model variability in simulating temperature trends. This is quantified by grouping the models by their treatment of ozone changes as summarized in Table 1 above (i.e., AOGCMs-O_3,

AOGCMs-NO_3 and CCMs) and then computing the standard deviation of the trend within each model group, as shown in Fig. 3. Models with a higher standard deviation indicate that there is large model-to-model variability among the group of models.

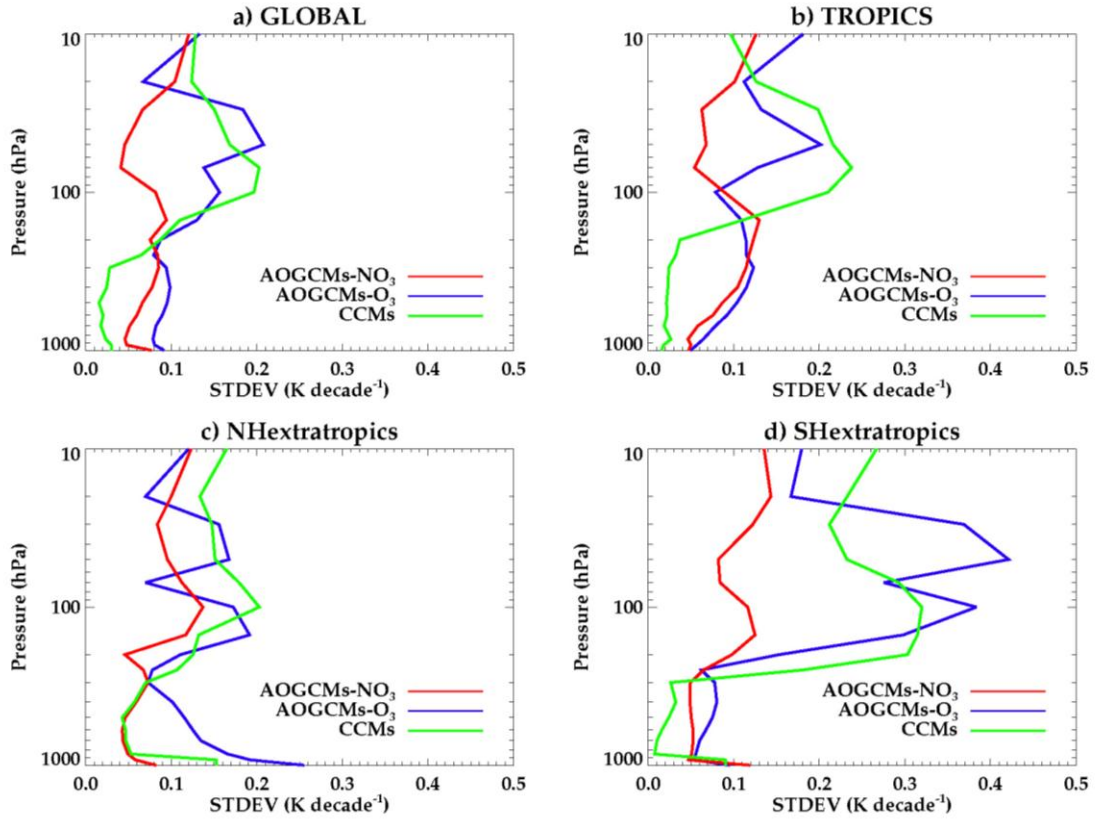

Fig. 3. Annual model-to-model variability as a function of pressure for 1980-2004. Averaged CCMs, AOGCMs-O_3 and AOGCMs-NO_3 are represented by green, blue, and red solid lines, respectively.

The results show significantly larger intermodel variability in the stratosphere than in the troposphere in all four regions for the AOGCMs-O_3. In addition, model variability is generally largest for the AOGCMs-O_3 and smallest for the AOGCMs-NO_3 in the stratosphere for all regions. For example, the annual global standard deviation at 50 hPa from the averaged AOGCMs-O_3 and averaged CCMs (Fig. 3a) is about 0.21 K

decade^{-1} and 0.17 K decade^{-1}, respectively while the averaged AOGCMs-NO_3 shows a standard deviation close to zero (0.05 K decade^{-1}). The largest standard deviation from averaged models is found in the SHextra lower stratosphere, particularly at 100 hPa where both the averaged CCMs (0.32 K decade^{-1}) and AOGCMs-O_3 (0.38 K decade^{-1}) have greater standard deviation compared to the AOGCMs-NO_3 (0.12 K decade^{-1}). This is likely associated with the large model-to-model differences in the representation ozone trends in the SHextra. For example, in the CCM simulations shown in Eyring et al. (2006), the size of ozone trends in the SHextra varied by about 30% percent.

In the troposphere, the averaged CCMs generally show the smallest standard deviation, compared to the averaged AOGCMs. For example, the standard deviation for the annual global mean temperature at 500 hPa from the averaged CCMs show 0.02 K decade^{-1} while the averaged AOGCMs-O_3 and AOGCMs-NO_3 show 0.10 K decade^{-1} and 0.07 K decade^{-1}, respectively. A likely explanation for this is that the CCMs use the identical time-varying prescribed sea surface temperatures (SSTs) in their simulations, while the AOGCMs use a fully coupled atmosphere ocean global circulation model. In the CCM simulations presented here, the SSTs were derived from satellite and in situ observations (Eyring et al. 2006) and thus the oceans which largely drive the troposphere, produce much larger model-to-model variability.

Figure 4 shows the vertical distribution of temperature trends as in Fig. 2 where models are grouped based on their inclusion of ozone forcing, allowing a more simple comparison of the model groups. In the stratosphere, the annual mean temperature for the averaged AOGCMs-O_3 and CCMs appear to agree well with radiosonde observations

while the averaged AOGCMs-NO_3 appears outside the observational trends. For example, in the global and tropics, averaged AOGCMs-NO_3 show annual mean temperature trends that appear larger than observed between 150 hPa and 30 hPa while in the NHextra, the averaged AOGCMs-NO_3 show larger trends than observed between 70 hPa and 30 hPa. The largest trend difference between averaged AOGCMs-NO_3 and observations are seen in the SHextra between 100 hPa and 50 hPa. This indicates that changes in the stratospheric ozone play an important role in simulating stratospheric temperature.

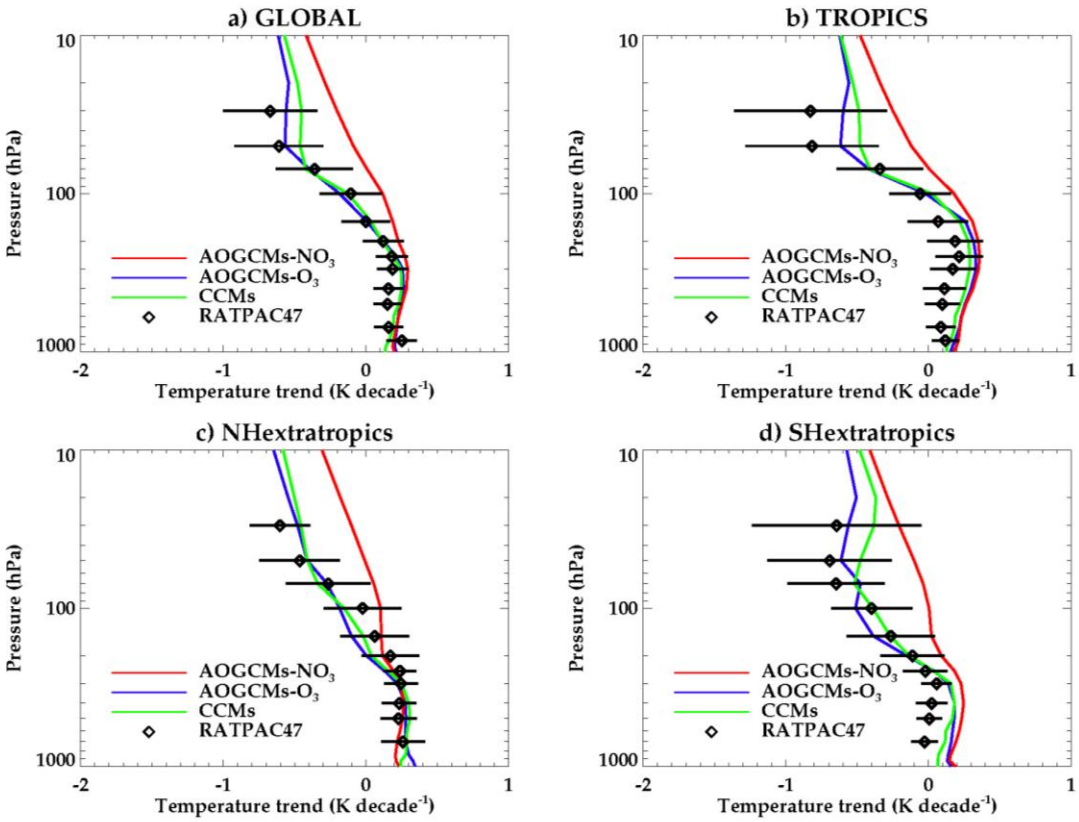

Fig. 4. As in Fig. 2 but the trends are calculated from the grouped and averaged models. Averaged CCMs, AOGCMs-O_3 and AOGCMs-NO_3 are represented by green, blue, and red solid lines, respectively. The radiosonde observations are represented by black diamond symbols.

In the troposphere, averaged AOGCMs-NO_3 generally show larger annual mean temperature trends compared to observations. And in the tropics between 300 and 500 hPa, only averaged CCMs appear to agree with radiosonde observations (i.e., while models show warming, observations shows less warming in the tropics). In the NHextra, each averaged models (i.e., AOGCMs-O_3, AOGCMs-NO_3 and CCMs) and observations generally show better agreement in the annual mean temperature trends. However, in the SHextra between 300 and 500 hPa pressure levels, the averaged models appear to disagree with radiosonde observations (i.e., observations show almost no warming in the SHextra), similar to Fig. 2d. Further analysis comparing each averaged models and individual model with the observations is presented below in Section b.

Figure 4 also illustrates the difference between models and observations regarding the location of the transition between warming and cooling trends, herein referred to as "crossover". Table 3 summarizes the location of the crossover for both models and observations. Both groups of ozone models (AOGCMs-O_3 and CCMs) and observations show crossover altitudes at 150 hPa in the global mean. However, in the tropics and NHextra, the ozone models and observations do not fully agree in the crossover altitudes. For example, in the NHextra, observations show a crossover altitude at 100 hPa whereas ozone models show a crossover at 150 hPa. The AOGCMs-NO_3 show consistently high results (by 2-8 km) in the crossover point. The location of the crossover point seems to be sensitive to the inclusion of ozone forcing and the CCMs and AOGCMs-O_3 show very similar results. Moreover, the effect of model resolution to the crossover location were investigated by categorizing the AOGCMs-O_3 into two groups, where AOGCMs-O_3 with

high and low resolution are referred as AOGCMs-highO_3 and AOGCMs-lowO_3, respectively. We found the location of the crossover to be insensitive to the vertical resolution (not shown).

Table 3. Crossover location for both models and radiosonde observations in four latitude bands (global, 90N-90S, tropics, 30N-30S, NHextra, 30N-90N, SHextra, 30S-90S). The location is expressed in term of pressure (hPa). Ozone models include CCMs and AOGCMs-O_3.

	Global (90^oS-90^oN)	Tropics (30^oS-30^o N)	NHextra (30^oN-90^oN)	SHextra (30^oS-90^oS)
Ozone models	150	100	150	250
AOGCMs-NO_3	70	70	50	150
Radiosonde observations	150	Between 150 and 100	100	250

Another characteristic difference between models and observations is related to the vertical distribution of temperature trends, especially in the troposphere. For example, observational temperature trends between 850 and 250 hPa are approximately constant with height, while models show increasing temperature trends with height from the surface to 300 hPa in the global mean. Similar differences between models and observations are found in both the tropics and the SHextra. Santer et al. (2005) suggest that the greater warming aloft in the upper tropical troposphere in models is connected with the moist adiabatic ascent of convective air parcels. In addition, the different rate of warming aloft among models may be associated to the difference in the convective and/or radiation scheme used in the climate models (Forster et al. 2001). However, in the

NHextra, both models and observations show nearly constant temperature trends with height from surface through ~300 hPa and thus the difference between hemispheres is unclear.

A further comparison of models and observations is facilitated by comparing trends in the NHextra with trends in the SHextra. Figure 5 shows simulated and observed annual temperature trend differences between the NHextra and the SHextra from the surface through 10 hPa. The largest hemispheric trend differences are found at 100 hPa, where observations show a 0.48 K decade^{-1} larger trend in the NHextra compared to the SHextra.

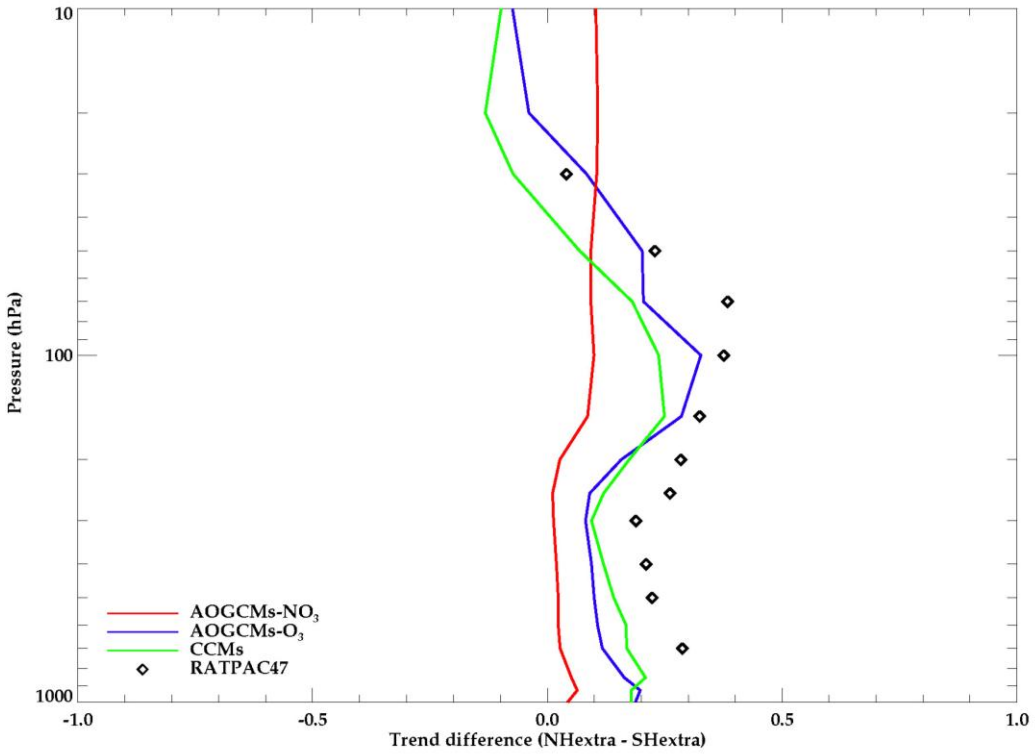

Fig. 5. Annual trend differences in K decade^{-1} between northern and southern hemisphere extratropics for the averaged AOGCMs-O_3 (blue solid line), AOGCMs-NO_3 (red solid line), CCMs (green solid line) and radiosonde observations (black diamond symbols).

Based on Fig. 5, this is at least partially explained by additional cooling in the SHextra due to enhanced ozone depletion. Similarly, the ozone models (AOGCMs-O_3, and CCMs) show a larger SHextra cooling trends (by 0.33 K decade^{-1}, and 0.23 K decade^{-1}, respectively), compared to the NHextra. In addition, larger cooling from ozone models is simulated in the NHextra, compared to the SHextra at 20 hPa and 10 hPa, where there are no reliable radiosonde measurements to compare with the models. The AOGCMs-NO_3 show nearly constant hemispherical trend differences from surface to 10 hPa, while the ozone models are much closer to the observed trend difference between NHextra and SHextra. Statistically significant hemispherical trend differences between AOGCMs-NO_3 and AOGCMs-O_3 are found between 300 hPa and 850 hPa (see Table 4).

Table 4. Statistical comparison between the groups of models based on hemispherical trend differences.

Pressure	AOGCMs-O_3 minus AOGCMs-NO_3	AOGCMs-O_3 minus CCMs	AOGCMs-NO_3 minus CCMs
10	Yes	No	Yes
20	Yes	No	Yes
30	No	No	No
50	Yes	No	No
70	No	No	No
100	Yes	No	No
150	Yes	No	No
200	Yes	No	No
250	No	No	No
300	Yes	No	No
400	Yes	No	No
500	Yes	No	Yes
600	Yes	No	Yes
700	Yes	No	Yes
850	Yes	No	Yes
925	No	No	No
1000	No	No	Yes

Although one would expect ozone models to better agree with observations in the stratosphere, these results suggest that stratospheric ozone change may affect trends in the troposphere.

c. Temperature trend comparisons between models and observations

While a visual comparison of the model trends with observations provides insight into how well the models agree with observations, a statistical comparison of each model or group of models with the observations is required to determine if the trends are statistically consistent with the observations. As mentioned in the methodology section, the agreement between models and observations are defined based on the calculated trends from the time series difference between models and observation. If the trends from the time series difference between models and observation are statistically significant at 95 % confidence level, then there is a real difference between models and observations. Likewise models and observations agree when the trends from the time series difference is not statistically significant at 95 % confidence level.

1) Annual trends

Overall, individual model and RATPAC47 observations agree reasonably well in the troposphere and stratosphere in the annual mean temperature, although there are differences. Figure 6a generally shows good agreement in the global annual mean temperature trend between RATPAC47 and both CCMs and AOGCMs-O_3 in the four regions at 50 hPa, while the AOGCMs-NO_3 do not agree with the observations. The trends from the AOGCMs-NO_3 are statistically warmer than the RATPAC47 trends in the

global annual mean, tropics and NHextra (except CNRM-CM3 and IPSL-CM4). For example, global annual mean temperature trends at 50 hPa from the RATPAC47 datasets show a statistically significant cooling trend of -0.61 K decade^{-1}. Almost all CCMs (5/7) [-0.27 to -0.72 K decade^{-1}], and AOGCMs-O_3 (6/8) [-0.30 to -0.89 K decade^{-1}] agree with RATPAC47 trends while all AOGCMs-NO_3 underestimate the lower stratospheric cooling trend (0.52 K decade^{-1}, not shown) with the trend values that range between ~ -0.05 K decade^{-1} and -0.11 K decade^{-1}. Similar results are found in the tropics and NHextra such that the ozone models generally agree with observations and the AOGCMs-NO_3 have trends that are statistically different from the observations.

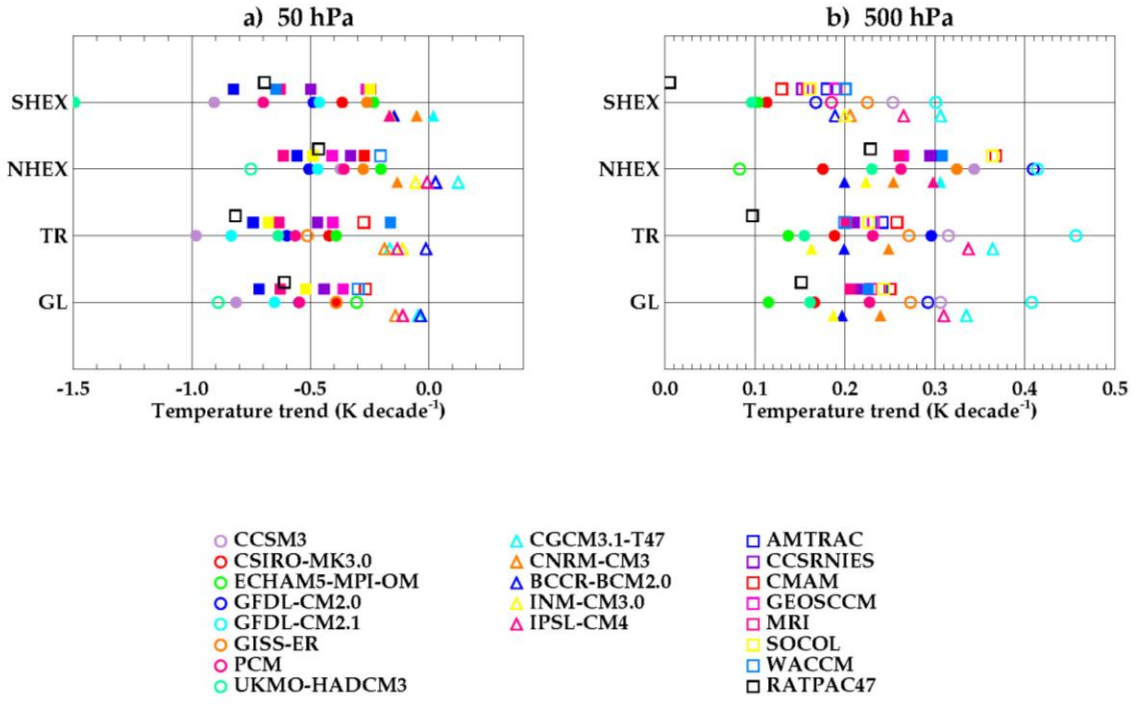

Fig. 6. Annual temperature trend comparisons between each model and radiosonde observations in four regions at a) 50 hPa and b) 500 hPa pressure levels. The AOGCMs-O_3, AOGCMs-NO_3, and CCMs are represented by colored circle, triangle and square symbols. Shaded symbols indicate the agreement between models and radiosonde observations.

These results agree with Cordero and Forster (2006) who observed differences between AOGCMs-NO_3 and observations in the upper troposphere and lower stratosphere in the global and tropics for AOGCMs.

The largest differences between models and observations are found in the middle troposphere (500 hPa), where there is poor agreement between all models and observations, especially in the SHextra (Fig. 6b). Observations of the trends in the SHextra show almost no warming (0.01 K decade^{-1}), while CCMs show warming (between 0.13 K decade^{-1} and 0.20 K decade^{-1} with an average of 0.16 K decade^{-1}), AOGCMs-O_3 (between ~ 0.1 K decade^{-1} and 0.30 K decade^{-1}) and AOGCMs-NO_3 (between 0.14 K decade^{-1} and 0.31 K decade^{-1}). Inspection of the trends in the SHextra finds that only three models (UKMO-HADCM3, ECHAM5-MPI-OM, and CSIRO-MK3.0) actually agree with the observed temperature trends. Although it has been suggested (Lanzante and Free 2008) that the weak observed trends in the SHextra may be related to the scarcity of radiosonde data, as seen in the satellite section (Section 3), the radiosonde observed trends appear to be in agreement with the satellite observations. In the tropics and NHextra, although the observed trends at 500 hPa are larger than most of the model trends, the trends are statistically similar.

2) Seasonal trends

To further explore the trend differences between models and observations, seasonal trends are computed at 50 hPa and 500 hPa pressure levels and four latitude bands (global, tropics, NHextra and SHextra) for the averaged models and observations.

Figures 7a-d show seasonal trends in the lower stratosphere at 50 hPa, while Figs. 8a-d shows seasonal trends in the middle troposphere.

(i) Lower stratosphere (50 hPa) trends

In the global mean at 50 hPa, the strongest observed cooling is found during SON, where the ozone models seem to match the observed trends fairly well, while the AOGCMs-NO_3 models show little seasonal variability in the trend (Fig. 7a). Although reasonable agreement exists between the ozone models and observations for the global mean, in the different regions the observed seasonal trend variation is not well simulated in any of the model groups. In the tropical annual mean (Fig. 7b), the models underestimated the observed cooling trend (-0.82 K decade^{-1}) and do not show the observed seasonal trend variation. Further seasonal temperature trend comparison between individual models and radiosonde observations is made at 50 hPa (not shown). A few models (ECHAM5-MPI-OM, GFDL-CM2.0, SOCOL and MRI) show seasonal tropical temperature trend variations that resemble to the radiosonde observations.

The seasonal tropical stratospheric temperature trends from observations (RATPAC47) show much larger cooling during DJF and SON, compared to MAM and JJA. These results agree with the findings of Free et al. (2005) who used RATPAC-A for stratospheric layer means (100-50 hPa) over the period 1979-2004. At least at 50 hPa, this indicates that DJF and SON play a major role on the annual tropical temperature trends. Temperature trends in the tropical stratosphere are controlled both by local heating due to changes in GHGs and changes in ozone (Forster et al. 2001), and externally by changes in the Brewer Dobson circulation (Li et al. 2008). Thus, the

tropical seasonal trend difference between models and observations indicates that the observed enhanced cooling in the DJF and SON is apparently not related to ozone changes since neither the ozone models nor AOGCMs-NO_3 show any seasonality. It is possible these seasonal cooling trends are related to circulation changes (e.g., changes in the Brewer Dobson circulation (Butchart et al. 2009), although this remains unclear).

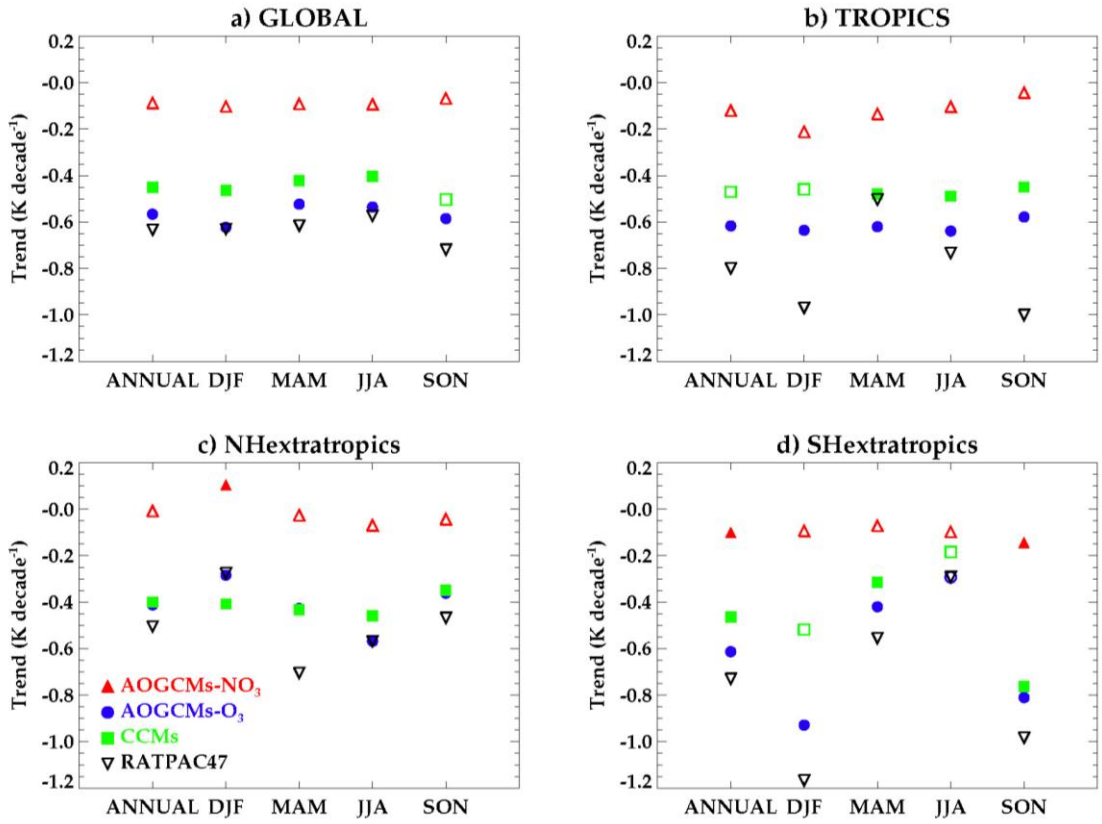

Fig. 7. Annual and seasonal temperature trends for the grouped and averaged models and radiosonde observations at 50 hPa. The averaged AOGCMs-O_3, AOGCMs-NO_3, CCMs and radiosonde observations are represented by blue circles, red upward triangles, green squares, and downward black triangles, respectively.

In the NHextra a reasonably large seasonal trend variation is also observed, and yet the models do not show such a strong variation (Fig. 7c). The MAM season has the coolest trends from observations, but this feature is not resolved in the models. However, the largest seasonal variations are found in the SHextra, where DJF and SON show by far the coolest trends (Fig. 7d). In this case, the ozone models do a better job resolving the observed seasonal variations, and these variations appear to be related primarily to ozone variations.

(ii) Middle troposphere (500 hPa) trends

For global mean temperatures at 500 hPa (Fig. 8a), all models generally agree with observations in the annual mean and during all four seasons (i.e., DJF, MAM, JJA and SON seasons). At the tropical middle troposphere (500 hPa), none of the models agree with the observations in the annual mean (Fig. 8b). While a statistical agreement between models and observations is found during MAM and SON, the model trends are significantly different from observations during DJF and JJA. Furthermore, in the tropics the averaged models show warmer temperature trends than the radiosonde observations during all seasons, while in the NHextra, the observed and modeled seasonal trend variations are generally in good agreement (Fig. 8c).

The most striking difference is, however, found in the SHextra middle troposphere (500 hPa), where in the annual and MAM/JJA, none of the averaged models agree with the observed trends (Fig. 8d). The radiosonde observations show a moderate seasonal trend variation with weak cooling in MAM and JJA. As we will illustrate in the next section, these results generally agree with satellite data. Both CCMs and AOGCMs-

O_3 agree with observations only during DJF and SON, but during MAM and JJA, cooling trends are shown in the observations while all models show warming. In Fig. 5, we observed the large differences between the hemisphere trends and the observations in the troposphere, and that analysis suggested that ozone models better agree with observations from the stratosphere to the troposphere. Even so, there still appears a statistical difference between models and observations in the SHextra, the origin of this difference at present is unclear.

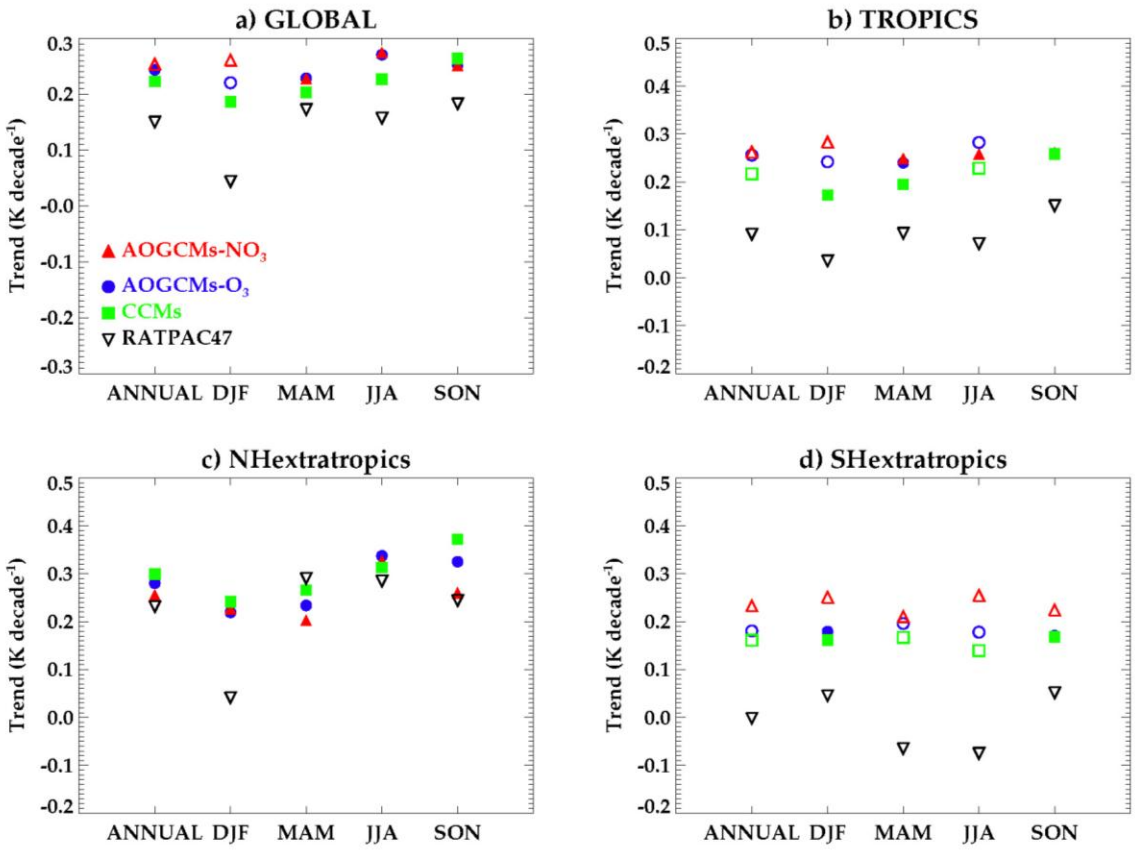

Fig. 8. As in Fig. 7 except for 500 hPa. Note that in a few cases, the symbols denoting the ozone models (e.g. AOGCM-O_3) have been obscured by the square symbol for the CCMs.

3) Satellite comparisons

To confirm the results comparing models with radiosonde observations, we now repeat some of the above analysis using the satellite record. Figures 9 show the layer averaged annual and seasonal TMT and TLS trends from the grouped and averaged models compared with the satellite and RATPAC47 observations in the four regions (i.e., global, tropics, NHextra and SHextra) during the 1980-2004 period.

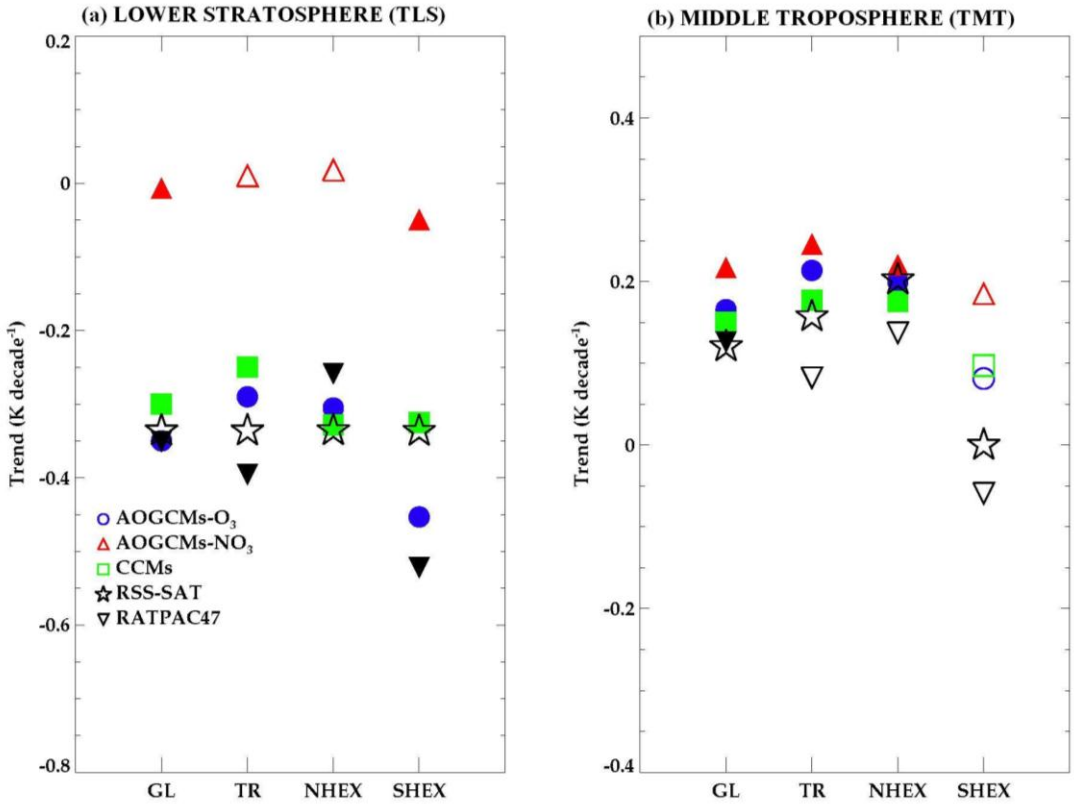

Fig. 9. Annual layered temperature trends for (a) lower stratosphere (TLS) and (b) middle troposphere (TMT) from the grouped AOGCMs-O_3 (blue circles), AOGCMs-NO_3 (red upward triangles), and CCMs (green squares), plus the MSU4 (black stars), and RATPAC47 (black downward triangles) for global, tropics, northern and southern hemisphere extratropics during 1980-2004 period. Trends from the time series differences between models and satellite observation are evaluated to examine if there is a statistically significant difference (at 95 % confidence level) between models and observation. Shaded symbols indicate the agreement between models or radiosonde and satellite observations.

In general, while the ozone models show reasonable agreement with the satellite and radiosonde observations, there are differences found both between the two observational datasets and in comparing the models with observations. In the global annual mean TLS (Fig. 9a), the satellite and radiosonde observations are in close agreement showing a cooling of around -0.35 K decade^{-1}. However, in three different regions (i.e., tropics, NHextra and SHextra), there are significant differences. The satellite observations show nearly uniform cooling trends at the three regions while the radiosonde observations show larger cooling trends in the SHextra and tropics compared to the NHextra. The AOGCMs-O_3 tend to agree with the radiosonde observations showing much larger cooling in the SHextra compared to the NHextra, while the CCMs agree well with the satellite data, showing essentially no difference in trends between the NHextra and the SHextra.

Further insights into the differences found in the lower stratosphere are explored using the seasonal TLS temperature trends as shown in Fig. 10 and confirm results obtained by comparing models with radiosonde observations in the stratosphere (Fig. 7a-d). More specifically, although there are differences in the observed trends especially in DJF and SON, the structure of the seasonal variation in the extratropical trends is well represented in both satellite and radiosonde observations. In the NHextra, both observations show the coldest trends in MAM and the warmest in DJF, while in the SHextra, the coldest trends are during DJF and the warmest during JJA. The stronger cooling trends in both hemisphere extratropics appear to follow the larger ozone

depletion season. In both cases, radiosonde observations show a significant larger seasonal trend variation than the satellite observation.

In the NHextra, the models again underestimate the magnitude of the observed seasonal variations in trends. Although the AOGCMs-O_3 shows some seasonal variation, the CCMs and AOGCMs-NO_3 almost show no seasonal variation in trends. For the AOGCMs, this could be understood by how the inclusion of ozone forcing is incorporated. In most modeling groups, the change in ozone is applied uniformly throughout the year at each latitude, and thus the seasonal variation in temperature trends due to changes in ozone would not be resolved. However, for the CCMs, we would expect to see realistic seasonal variations in trends, and although we do see some trend differences in the SHextra, its magnitude is much smaller than observed, while in the NHextra, there is essentially no seasonal variation. In the tropical stratosphere, for both the observed trends, DJF and SON show the strongest cooling trends, while during MAM are the weakest cooling trends. And, for all groups of models, no seasonal variations in the tropical trends are found. Interestingly, the satellite trends show larger seasonal variations compared to the radiosonde trends; the opposite of what we saw in the extratropics.

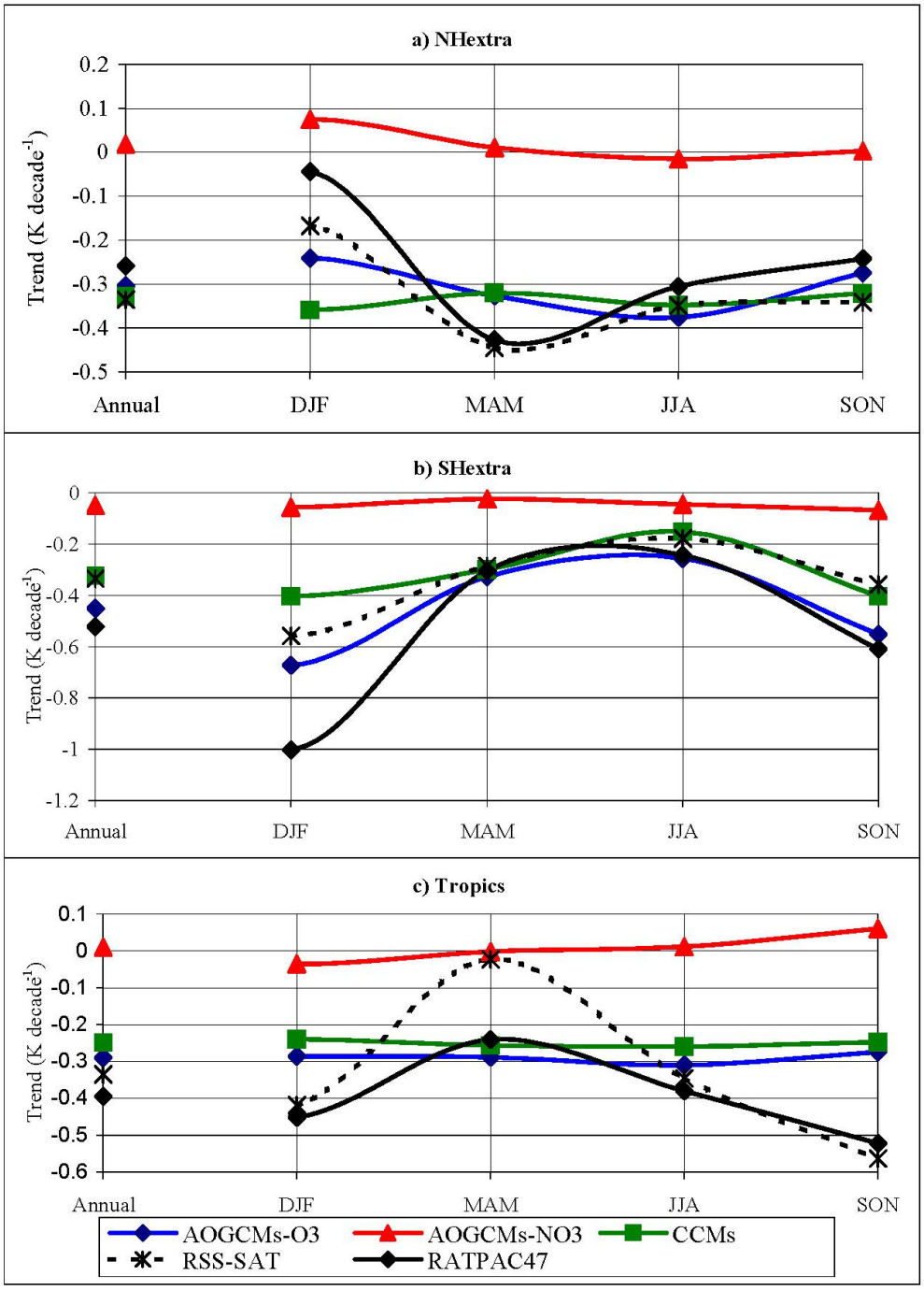

Fig. 10. Observed and simulated seasonal TLS trends in three latitude bands (tropics, NHextra, and SHextra). The seasonal trends from averaged AOGCMs-O_3, AOGCMs-NO_3 and CCMs are represented by blue, red and green lines whereas satellite and radiosonde seasonal trends are represented by black dashed and solid lines, respectively.

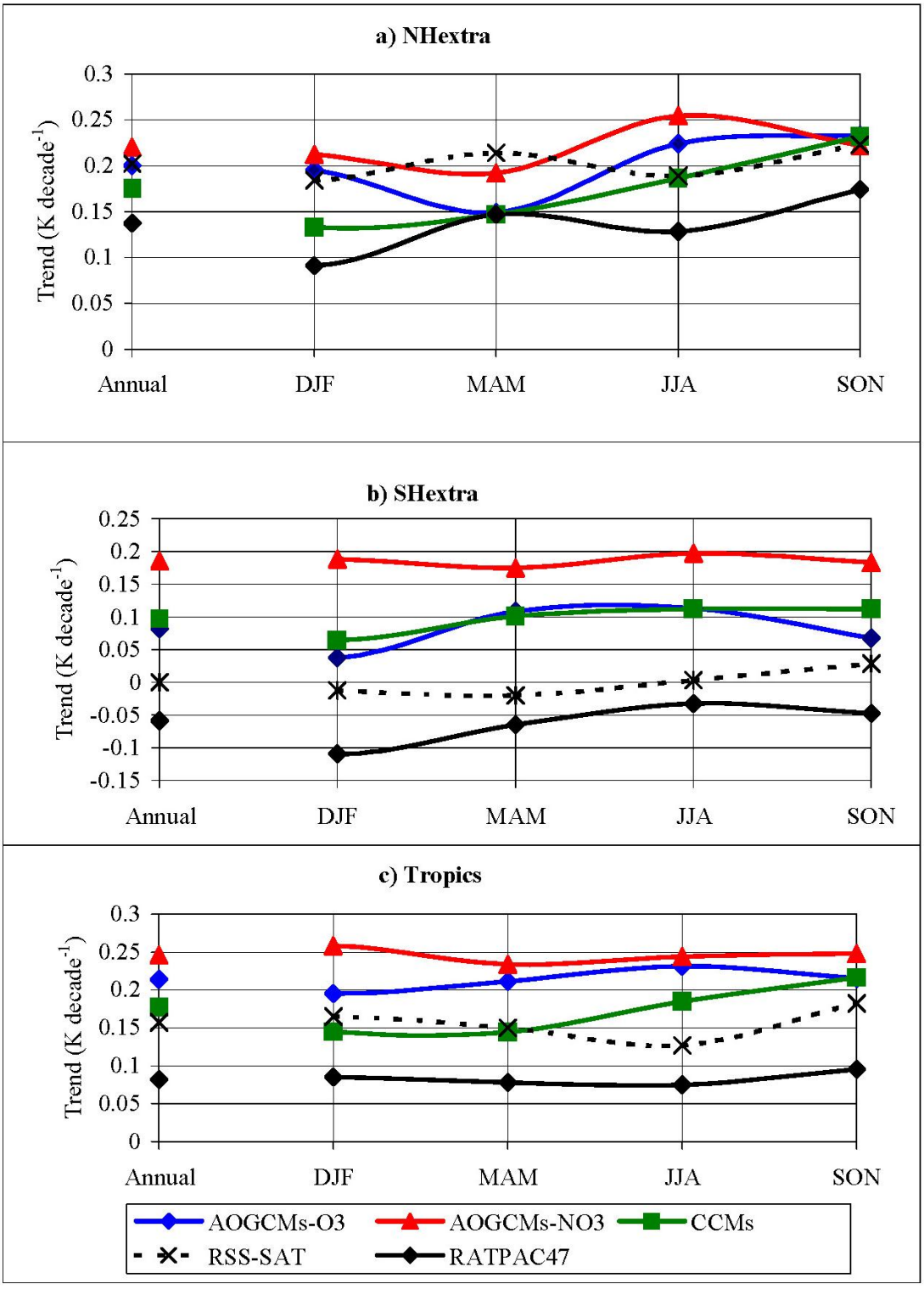

Fig. 11. As in Fig. 10 except for TMT layered trends.

A comparison in the layer averaged TMT using the satellite data is also consistent with the previous comparison using the radiosonde data (Fig. 11). The models generally agree with satellite data in the annual mean temperature trends in all regions except in the SHextra, where all the models show a warming trend in the middle troposphere while the radiosonde and satellite observations show significantly cooler trends (Fig. 9b). The seasonal variations in tropospheric trends (Fig. 11) reveal the following. The largest difference between the models and observations is found in the SHextra, where both the radiosonde and satellite trends are significantly weaker than the models. In the tropics, the observed trends are also generally smaller in magnitude than the modeled trends, while in the NHextra, the modeled and observed trends are in reasonable agreement, at least in terms of the magnitude. In the case of the SHextra and tropics, the AOGCMs-NO_3 trends are consistently warmer than the other modeled trends and observed trends.

d. Analysis of southern hemisphere trends

To further explore the large difference between models and observations in SHextra, a correlation analysis between observational based southern hemisphere annular mode (SAM) index and temperature trends from models and radiosonde observations were performed over the period 1980-2004. The method of analysis of the observational SAM index has been described by Marshall (2003) and the dataset are updated on monthly base. The correlation between SAM index and temperature are summarized in Table 5 and Table 6 for both SHextratropical (30^oS-90^o S) and SH polar (60^oS-90^o S) regions, respectively and found the following. A negative correlation between the annual

SAM index and temperature are observed from 200 hPa through 70 hPa in both SHextra and SH polar regions, which are statistically significant at 95 % confidence level. Contrary to AOGCMs, CCMs also show a reasonably negative correlation (statistically significant) between annual SAM index and temperature above 200 hPa. This might indicate that CCMs better able to capture the troposphere-stratosphere coupling than the AOGCMs.

Table 5. Correlation between the annual observational SAM index and annual SHextratropical temperature. The correlation values that are statistically significant at the 95 % confidence level are represented in bold.

Pressure	AOGCMs-O_3	AOGCMs-NO_3	CCMs	RATPAC47
10	**-0.406**	**-0.438**	**-0.467**	N/A
20	**-0.415**	**-0.448**	**-0.427**	N/A
30	-0.389	**-0.428**	**-0.421**	-0.411
50	-0.384	-0.391	**-0.448**	-0.272
70	-0.391	-0.276	**-0.469**	**-0.723**
100	-0.342	-0.079	**-0.508**	**-0.784**
150	-0.321	-0.074	**-0.504**	**-0.772**
200	-0.272	0.024	**-0.458**	**-0.612**
250	0.080	0.241	-0.180	-0.258
300	0.248	0.286	0.142	0.129
400	0.285	0.313	0.238	N/A
500	0.299	0.335	0.249	-0.127
600	0.318	0.354	0.214	N/A
700	0.323	0.341	0.213	-0.337
850	0.342	0.251	0.089	N/A
925	0.363	0.209	-0.153	N/A
1000	0.312	0.244	-0.142	N/A

Table 6. Same as Table 5 except for annual SAM index versus SH polar region temperature correlation.

Pressure	AOGCMs-O_3	AOGCMs-NO_3	CCMs	RATPAC47
10	-0.359	-0.375	**-0.520**	N/A
20	-0.398	-0.367	**-0.446**	N/A
30	-0.371	-0.363	**-0.439**	-0.007
50	-0.387	-0.355	**-0.465**	-0.096
70	-0.396	-0.329	**-0.485**	**-0.669**
100	-0.378	-0.299	**-0.494**	**-0.668**
150	-0.385	-0.382	**-0.463**	**-0.672**
200	**-0.414**	-0.407	**-0.426**	**-0.595**
250	**-0.437**	-0.157	**-0.422**	-0.359
300	-0.168	0.096	-0.280	-0.013
400	0.214	0.190	-0.041	-0.179
500	0.294	0.228	-0.001	-0.339
600	0.360	0.222	-0.063	N/A
700	0.351	0.158	-0.059	-0.489
850	0.345	0.029	-0.148	N/A
925	0.325	-0.006	-0.283	N/A
1000	0.053	-0.105	-0.277	N/A

4. Discussion and summary

The simulated annual and seasonal temperature trends from a subset of AOGCMs and CCMs were compared with radiosonde and satellite observations. The comparisons were carried out on four latitude bands (i.e., global, tropics, NHextra, and SHextra) and both the TMT and TLS from the surface through 10 hPa. The core period of the temperature trend comparison between models and observations is from 1980 to 2004. Models and observations generally showed similar annual mean vertical temperature profiles, with warming in the troposphere and cooling in the stratosphere in all four regions. More specifically, although some models showed a warm (GFDL-CM2.0 and GFDL-CM2.1) or cold (Echam-hadcm3, AMTRAC and MRI) bias, the averaged models

agreed with the radiosonde and satellite observations. It is suggested that cold biases in the stratosphere from AMTRAC and MRI models are related to the lack of accurate simulations for the observed ozone anomalies (Eyring et al. 2006), while the troposphere warming biases result from the larger ENSO amplitude (Lanzante and Free 2008).

Further temperature trend analysis was conducted by grouping models based on their inclusion of ozone forcing (AOGCMs-O_3 and AOGCMs-NO_3) and type of coupling used (CCMs), which facilitated model versus observation comparisons and highlighted the importance of ozone forcing in climate model simulations in the stratosphere. More specifically, only ozone models agreed reasonably well with radiosonde observations in the stratosphere, consistent with the Cordero and Forster (2006) findings. Ozone models showed similar crossover locations, while AOGCMs-NO_3 showed a crossover at higher altitudes, consistent with the Lanzante and Free (2008) findings where changes in crossover locations from both models and observations were found associated with the stratospheric cooling caused by ozone depletion. Nonetheless, these groups of models have a systematic difference in the prescribed ozone forcing as demonstrated by calculating the standard deviation among the groups of models. The calculations show that larger model-to-model variability exists in the stratosphere compared to the troposphere, especially in the SHextra where both CCMs and AOGCMs-O_3 showed the largest model-to-model variability. The larger model-to-model variability in the SHextra indicates the larger model variability in representing the ozone hole.

Another important feature of the vertical temperature trend analysis is the difference in the temperature trends between northern and southern hemisphere

extratropics. Both ozone models and observations showed trend differences between the northern and southern hemisphere extratropics, especially at 100 hPa, whereas AOGCMs-NO_3 failed to show these hemispheric temperature trends differences. This hemisphere difference suggests the importance of ozone forcing on the climate models' simulations, even down into the troposphere.

To confirm results obtained by comparing models with radiosonde observations, additional annual and seasonal comparisons of satellite observations with radiosonde observations and models in the lower stratosphere and middle troposphere were made. Our main findings are as follows. First, the AOGCMs-NO_3 have shortcomings, particularly in the stratosphere, where they have a warm bias in all four regions. In addition, they do not resolve the observed seasonal variation at all. In the troposphere, model simulated temperature trends are warmer than observed, especially in the SHextra during MAM and JJA.

Second, all models show deficiencies in the tropical stratosphere and middle troposphere. In the tropical stratosphere, observations show a strong seasonal trend variation, while no class of models captures the observed seasonal temperature variations. In the middle troposphere, models do not agree with observations in the tropics, especially during DJF and JJA. It is unclear why models do such a poor job replicating the observations in the tropical stratosphere and middle troposphere. In the SH extratropical middle troposphere, significant differences between models and observations are also found in the annual mean and during MAM and JJA seasons, although the cause of the differences remains unclear. Obviously, there are concerns

about the potential biases due to the method of satellite retrieval (e.g., Fu et al. 2004) and on the scarcity of radiosonde measurements in the southern hemisphere. If both (radiosonde and satellite) trends are biased towards cold, then observations and models may actually be in good agreement. However, should the observations hold up over time, then a real difference exists. And since the large differences that exist between the models and observations in the high latitude southern hemisphere are even larger for the models that do not include ozone forcing, then one might be inclined to look more closely at how ozone changes affect tropospheric trends in the SH extratropics.

References

Angell, J. K., 2000: Difference in radiosonde temperature trend for the period 1979-1998 of MSU data and the period 1959-1998 twice as long. *Geophys. Res. Lett.*, **27,** 2177-2180.

Austin, J., D. Shindell, S. R. Beagley, C. Bruhl, M. Dameris, E. Manzini, T. Nagashima, P. Newman, S. Pawson, G. Pitari, E. Rozanov, C. Schnadt, and T. G. Shepherd, 2003: Uncertainties and assessments of chemistry-climate models of the stratosphere. *Atmos. Chem. Phys.*, **3,** 1-27.

Butchart, N., I. Cionni, V. Eyring, D. W. Waugh, H. Akiyoshi, J. Austin, C. Bruehl, M. P. Chipperfield, E. Cordero, M. Dameris, R. Deckert, S. M. Frith, R. R. Garcia, A. Gettelman, M. A. Giorgetta, D. E. Kinnison, F. Li, E. Mancini, E. Manzini, C. McLandress, S. Pawson, G. Pitari, E. Rozanov, F. Sassi, T. G. Shepherd, K. Shibata, and W. Tian, 2009: Chemistry-Climate model simulations of 21st century stratospheric climate and circulations changes. *J. Geophys Res.***,** submitted.

Butchart, N., and A. A. Scaife, 2001: Removal of chlorofluorocarbons by increased mass exchange between the stratosphere and troposphere in a changing climate. *Nature*, **410,** 799-802.

Butchart, N., A. A. Scaife, M. Bourqui, J. de Grandpre, S. H. E. Hare, J. Kettleborough, U. Langematz, E. Manzini, F. Sassi, K. Shibata, D. Shindell, and M. Sigmond, 2006: Simulations of anthropogenic change in the strength of the Brewer-Dobson circulation. *Clim. Dyn.*, **27,** 727-741.

Christy, J. R., R. W. Spencer, and W. D. Braswell, 2000: MSU tropospheric temperatures: Dataset construction and radiosonde comparisons. *J. Atmos. Ocean. Technol.*, **17,** 1153-1170.

Cordero, E. C., and P. M. D. Forster, 2006: Stratospheric variability and trends in models used for the IPCC AR4. *Atmos. Chem. Phys.*, **6,** 5369-5380.

Eyring, V., N. Butchart, D. W. Waugh, H. Akiyoshi, J. Austin, S. Bekki, G. E. Bodeker, B. A. Boville, C. Bruhl, M. P. Chipperfield, E. Cordero, M. Dameris, M. Deushi, V. E. Fioletov, S. M. Frith, R. R. Garcia, A. Gettelman, M. A. Giorgetta, V. Grewe, L. Jourdain, D. E. Kinnison, E. Mancini, E. Manzini, M. Marchand, D. R. Marsh, T. Nagashima, P. A. Newman, J. E. Nielsen, S. Pawson, G. Pitari, D. A. Plummer, E. Rozanov, M. Schraner, T. G. Shepherd, K. Shibata, R. S. Stolarski, H. Struthers, W. Tian, and M. Yoshiki, 2006: Assessment of temperature, trace species, and ozone in chemistry-climate model simulations of the recent past. *J. Geophys. Res.*, **111,** doi:10.1029/2006JD007327.

Eyring, V., N. R. P. Harris, M. Rex, T. G. Shepherd, D. W. Fahey, G. T. Amanatidis, J. Austin, M. P. Chipperfield, M. Dameris, P. M. d. F. Forster, A. Gettelman, H.-F. Graf, T. Nagashima, P. A. Newman, S. Pawson, M. J. Prather, J. A. Pyle, R. J. Salawitch, B. D. Santer, and D. W. Waugh, 2005: A strategy for process-oriented validation of coupled chemistry-climate models. *Bull. Am. Met. Soc.*, **86,** 1117-1133.

Eyring, V., D. W. Waugh, G. E. Bodeker, E. Cordero, H. Akiyoshi, J. Austin, S. R. Beagley, B. A. Boville, P. Braesicke, C. Bruhl, N. Butchart, M. P. Chipperfield, M. Dameris, R. Deckert, M. Deushi, S. M. Frith, R. R. Garcia, A. Gettelman, M. A. Giorgetta, D. E. Kinnison, E. Mancini, E. Manzini, D. R. Marsh, S. Matthes, T. Nagashima, P. A. Newman, J. E. Nielsen, S. Pawson, G. Pitari, D. A. Plummer, E. Rozanov, M. Schraner, J. F. Scinocca, K. Semeniuk, T. G. Shepherd, K. Shibata, B. Steil, R. S. Stolarski, W. Tian, and M. Yoshiki, 2007: Multimodel projections of stratospheric ozone in the 21st century. *J. Geophys. Res.*, **112,** doi:10.1029/2006JD008332.

Forster, P. M. D., M. Ponater, and W. Y. Zhong, 2001: Testing broadband radiation schemes for their ability to calculate the radiative forcing and temperature response to stratospheric water vapour and ozone changes. *Meteorologische Zeitschrift*, **10,** 387-393.

Free, M., D. J. Seidel, J. K. Angell, J. Lanzante, I. Durre, and T. C. Peterson, 2005: Radiosonde Atmospheric Temperature Products for Assessing Climate (RATPAC): A new dataset of large-area anomaly time series. *J. Geophys. Res.*, **110,** doi:10.1029/2005JD006169.

Fu, Q., C. M. Johanson, S. G. Warren, and D. J. Seidel, 2004: Contribution of stratospheric cooling to satellite-inferred tropospheric temperature trends. *Nature*, **429,** 55-58.

Fyfe, J. C., G. J. Boer, and G. M. Flato, 1999: The Arctic and Antarctic oscillations and their projected changes under global warming. *Geophys. Res. Lett.*, **26,** 1601-1604.

Gaffen, D. J., M. A. Sargent, R. E. Habermann, and J. R. Lanzante, 2000: Sensitivity of tropospheric and stratospheric temperature trends to radiosonde data quality. *J. Clim.*, **13,** 1776-1796.

Gillett, N. P., and D. W. J. Thompson, 2003: Simulation of recent Southern Hemisphere climate change. *Science*, **302,** 273-275.

Hurrell, J. W., S. J. Brown, K. E. Trenberth, and J. R. Christy, 2000: Comparison of tropospheric temperatures from radiosondes and satellites: 1979-98. *Bull. Am. Meteorol. Soc.*, **81,** 2165-2177.

IPCC, 2007: *Climate Change 2007: The Physical Scientific Basis. Contribution of Working Group I to the Fourth Assessment Report of the Intergovernmental Panel on Climate Change* Cambridge University Press, 996 pp.

Karpechko, A. Y., N. P. Gillett, G. J. Marshall, and A. A. Scaife, 2008: Stratospheric influence on circulation changes in the Southern Hemisphere troposphere in coupled climate models. *Geophys. Res. Lett.*, **35,** doi:10.1029/2008GL035354.

Kushner, P. J., I. M. Held, and T. L. Delworth, 2001: Southern Hemisphere atmospheric circulation response to global warming. *J. Clim.*, **14,** 2238-2249.

Lanzante, J. R., and M. Free, 2008: Comparison of radiosonde and GCM vertical temperature trend profiles: Effects of dataset choice and data homogenization. *J. Clim.*, **21,** 5417-5435.

Lanzante, J. R., S. A. Klein, and D. J. Seidel, 2003a: Temporal homogenization of monthly radiosonde temperature data. Part I: Methodology. *J. Clim.*, **16,** 224-240.

Lanzante, J. R., S. A. Klein, and D. J. Seidel, 2003b: Temporal homogenization of monthly radiosonde temperature data. Part II: Trends, sensitivities, and MSU comparison. *J. Clim.*, **16,** 241-262.

Li, F., J. Austin, and J. Wilson, 2008: The strength of the Brewer-Dobson circulation in a changing climate: Coupled chemistry-climate model simulations. *J. Clim.*, **21,** 40-57.

Marshall, G. J., 2003: Trends in the southern annular mode from observations and reanalyses. *J. Clim.*, **16,** 4134-4143.

Mears, C. A., M. C. Schabel, and F. J. Wentz, 2003: A reanalysis of the MSU channel 2 tropospheric temperature record. *Journal of Climate*, **16,** 3650-3664.

Meehl, G. A., C. Covey, T. Delworth, M. Latif, B. McAvaney, J. F. B. Mitchell, R. J. Stouffer, and K. E. Taylor, 2007: The WCRP CMIP3 multimodel dataset - A new era in climate change research. *Bull. Am. Meteorol. Soc.*, **88,** 1383-1394.

Nathan, T. R., and E. C. Cordero, 2007: An ozone-modified refractive index for vertically propagating planetary waves. *J. Geophys. Res.*, **112,** doi:10.1029/2006JD007357.

Parker, D. E., M. Gordon, D. P. N. Cullum, D. M. H. Sexton, C. K. Folland, and N. Rayner, 1997: A new global gridded radiosonde temperature data base and recent temperature trends. *Geophys. Res. Lett.*, **24,** 1499-1502.

Pawson, S., K. Kodera, K. Hamilton, T. G. Shepherd, S. R. Beagley, B. A. Boville, J. D. Farrara, T. D. A. Fairlie, A. Kitoh, W. A. Lahoz, U. Langematz, E. Manzini, D. H.

Rind, A. A. Scaife, K. Shibata, P. Simon, R. Swinbank, L. Takacs, R. J. Wilson, J. A. Al-Saadi, M. Amodei, M. Chiba, L. Coy, J. de Grandpre, R. S. Eckman, M. Fiorino, W. L. Grose, H. Koide, J. N. Koshyk, D. Li, J. Lerner, J. D. Mahlman, N. A. McFarlane, C. R. Mechoso, A. Molod, A. O'Neill, R. B. Pierce, W. J. Randel, R. B. Rood, and F. Wu, 2000: The GCM-reality intercomparison project for SPARC (GRIPS): Scientific issues and initial results. *Bull. Am. Meteorol. Soc.*, **81,** 781-796.

Peterson, T. C., T. R. Karl, P. F. Jamason, R. Knight, and D. R. Easterling, 1998: First difference method: Maximizing station density for the calculation of long-term global temperature change. *J. Geophys. Res.*, **103,** 25967-25974.

Ramaswamy, V., and M. D. Schwarzkopf, 2002: Effects of ozone and well-mixed gases on annual-mean stratospheric temperature trends. *Geophys. Res. Lett*, **29,** doi:10.1029/2002GL015141.

Randel, W. J., K. P. Shine, J. Austin, J. Barnett, C. Claud, N. P. Gillett, P. Keckhut, U. Langematz, R. Lin, C. Long, C. Mears, A. Miller, J. Nash, D. J. Seidel, D. W. J. Thompson, F. Wu, and S. Yoden, 2009: An update of observed stratospheric temperature trends. *J. Geophys. Res.*, **114,** doi:10.1029/2008JD010421.

Randel, W. J., and F. Wu, 2006: Biases in stratospheric and tropospheric temperature trends derived from historical radiosonde data. *J. Clim.*, **19,** 2094-2104.

Randel, W. J., and F. Wu, 1999: Cooling of the arctic and antarctic polar stratospheres due to ozone depletion. *J. Clim.*, **12,** 1467-1479.

Rayner, N. A., D. E. Parker, E. B. Horton, C. K. Folland, L. V. Alexander, D. P. Rowell, E. C. Kent, and A. Kaplan, 2003: Global analyses of sea surface temperature, sea ice, and night marine air temperature since the late nineteenth century. *J. Geophys. Res.*, **108,** 4407, doi:4410.1029/2002JD002670.

Santer, B. D., J. J. Hnilo, T. M. L. Wigley, J. S. Boyle, C. Doutriaux, M. Fiorino, D. E. Parker, and K. E. Taylor, 1999: Uncertainties in observationally based estimates of temperature change in the free atmosphere. *J. Geophys. Res.*, **104,** 6305-6333.

Santer, B. D., R. Sausen, T. M. L. Wigley, J. S. Boyle, K. AchutaRao, C. Doutriaux, J. E. Hansen, G. A. Meehl, E. Roeckner, R. Ruedy, G. Schmidt, and K. E. Taylor, 2003a: Behavior of tropopause height and atmospheric temperature in models, reanalyses, and observations: Decadal changes. *J. Geophys. Res.*, **108,** doi:10.1029/2002JD002258.

Santer, B. D., M. F. Wehner, T. M. L. Wigley, R. Sausen, G. A. Meehl, K. E. Taylor, C. Ammann, J. Arblaster, W. M. Washington, J. S. Boyle, and W. Bruggemann, 2003b:

Contributions of anthropogenic and natural forcing to recent tropopause height changes. *Science*, **301,** 479-483.

Santer, B. D., T. M. L. Wigley, C. Mears, F. J. Wentz, S. A. Klein, D. J. Seidel, K. E. Taylor, P. W. Thorne, M. F. Wehner, P. J. Gleckler, J. S. Boyle, W. D. Collins, K. W. Dixon, C. Doutriaux, M. Free, Q. Fu, J. E. Hansen, G. S. Jones, R. Ruedy, T. R. Karl, J. R. Lanzante, G. A. Meehl, V. Ramaswamy, G. Russell, and G. A. Schmidt, 2005: Amplification of surface temperature trends and variability in the tropical atmosphere. *Science*, **309,** 1551-1556.

Shine, K. P., M. S. Bourqui, P. M. D. Forster, S. H. E. Hare, U. Langematz, P. Braesicke, V. Grewe, M. Ponater, C. Schnadt, C. A. Smiths, J. D. Haighs, J. Austin, N. Butchart, D. T. Shindell, W. J. Randel, T. Nagashima, R. W. Portmann, S. Solomon, D. J. Seidel, J. Lanzante, S. Klein, V. Ramaswamy, and M. D. Schwarzkopf, 2003: A comparison of model-simulated trends in stratospheric temperatures. *Q. J. R. Meteorol. Soc.*, **129,** 1565-1588.

Steig, E. J., D. P. Schneider, S. D. Rutherford, M. E. Mann, J. C. Comiso, and D. T. Shindell, 2009: Warming of the Antarctic ice-sheet surface since the 1957 International Geophysical Year. *Nature*, **457,** 459-462.

Thompson, D. W. J., J. C. Furtado, and T. G. Shepherd, 2006: On the tropospheric response to anomalous stratospheric wave drag and radiative heating. *J. Atmos. Sci.*, **63,** 2616-2629.

Thompson, D. W. J., and S. Solomon, 2002: Interpretation of recent Southern Hemisphere climate change. *Science*, **296,** 895-899.

Wigely, T. M. L., B. D. Santer, and J. R. Lanzante, 2006: Tempertaure trends in the lower atmosphere**,** Appendix A: Statistical issues regarding trends.

WMO, 2007: Scientific assessment of ozone depletion:2006. *Global ozone research and monitoring project* Report No. **50,** 572 pp., Geneva, Switzerland.